Biosensors and Bioelectronics 141 (2019) 111420

Contents lists available at ScienceDirect

Biosensors and Bioelectronics

journal homepage: www.elsevier.com/locate/bios

Fabrication of an efficient and sensitive colorimetric biosensor based on Uricase/ Th-MOF for uric acid sensing in biological samples

Arastoo Badoei-dalfard[a,*], Nasrin Sohrabi[a], Zahra Karami[a], Ghasem Sargazi[b]

[a] Department of Biology, Faculty of Sciences, Shahid Bahonar University of Kerman, Kerman, Iran
[b] Department of Nanotechnology, Graduate University of Advanced Technology, Kerman, Iran

ARTICLE INFO

Keywords:
MOF
Uric acid
Sensing
Peroxidase mimicking

ABSTRACT

Recently, nanomaterial-based artificial enzymes have expected abundant consideration because of cheap, accessibility, and respectable stability. In this study, we report a Th-MOF artificial peroxidase, which can oxidize 3,3,5,5-tetramethylbenzidine by hydrogen peroxide to yield a blue product. The catalytic behavior of Th-MOF tracked Michaelis–Menten equation and the affinity of this nanozyme to the substrate was higher than horseradish peroxidase as a natural enzyme. The absorbance value of oxidized TMB is linearly associated with the hydrogen peroxide concentration. Since, hydrogen peroxide is the oxidative end product of uric acid (UA) by uricase, an efficient and sensitive approach for uric acid determination was also established. Results showed that *K*m value of Th-MOF with TMB as a substrate is much lower than that of other mentioned catalysts. The linear regression equations for uric acid substrate was stated as A = 0.0039C + 0.0519 with a correlation coefficient of 0.9955. The linear range for uric acid was from 4.0 to 70 μM, and the LOD was measured as 1.15 μM. Furthermore the absorbance of assay reaction was approximately constant in the following four cycles, demonstrating that Th-MOF catalyst has outstanding stability. Results showed that the public interfering substances had no obvious absorbance values and it was less than 0.1. Results indicated that the recoveries for UA in serum fluids were between 93.10% and 99.04%. The relative standard deviation (RSD, n = 3) at each concentration value was less than 4.3%. UA determination in serum fluids has been confirmed through a comparison between the recommended technique and tedious clinical approaches. Good recovery and accuracy of UA measurement indicated that this established colorimetric sensing system is appropriate for UA revealing in actual experimental samples.

1. Introduction

Uric acid (2,4,6-trihydroxypurine) is the primary final compound of purine nucleotide byproducts in human metabolism (Kand'a' r et al., 2006; Grabowska et al., 2008). For a healthy one, the usual value of uric acid in serum fluids is in the variety of 0.12–0.46 mM and in the variation of 1.4–4.5 mM in urinary secretion (Azmi et al., 2015). The unusual uric acid concentration in serum and urine samples is an indicator of some diseases such as renal disease (Nakagawa et al., 2006), gout (Falasca, 2006; Merriman, and Dalbeth, 2011) and Lesch–Nyhan syndrome (Nyhan, 1997). Consequently, measurement of uric acid in biological fluids is a systematic test in medical laboratories. In hyperuricemia, extreme values of uric acid are present in serum fluid. It has been stated that hyperuricemia to be related with metabolic syndrome (Lohsoonthorn and Dhanamun, 2006), hypertension (Cannon et al., 1966; Jossa et al., 1994), kidney stones, and cardiovascular diseases (Fang and Alderman, 2000; Dawson and Walters, 2006; Montagnana et al., 2008; Gagliardi et al., 2009), whereas aberrantly low value of UA in serum fluid may undergo from multiple sclerosis (Moccia et al., 2015) or Parkinson's disease (Shen et al., 2013). Furthermore it is also associated with other bodily defects such as diabetes, obesity, high cholesterol value, heart and kidney diseases (Johnson et al., 2003; Bainbridge and Roberts, 2008; Gagliardi et al., 2009; Rocha and Rocha, 2010).

Therefore, find a fast and reliable method for uric acid measurement is a critical necessity for disease treatment and diagnosis. Up to now, numerous analytical approaches for uric acid sensing in biological fluids have been described such as spectrophotometry methods, capillary electrophoresis method (CE) (Boughton et al., 2002; Zinellu et al., 2004; Matějčková et al., 2007), chemiluminescence approach (Zhang et al., 2014; Chaudhari et al., 2012), electrochemistry technique (Chauhan and Pundir, 2011; Kumar and Shanmugam, 2011; Liao et al.,

* Corresponding author.
E-mail address: badoei@uk.ac.ir (A. Badoei-dalfard).

https://doi.org/10.1016/j.bios.2019.111420
Received 11 February 2019; Received in revised form 23 May 2019; Accepted 6 June 2019
Available online 11 June 2019
0956-5663/

2014), fluorescence procedure, high pressure liquid chromatography (HLPC) (Wang et al., 2016; Jen et al., 2002; Perelló et al., 2005; Zhao, 2013; Zhou et al., 2013). In spite of that, these approaches encompass expensive components and instruments, intricate sample pretreatment, interface with similar compounds and finally arduous and time-consuming. Therefore, it is required to develop fast, efficient, simple, precise and sensitive approaches for the uric acid detection in the biological samples.

Recently, colorimetric chemosensors based on nanomaterial have fascinated broad consideration for researchers. No necessity for any sophisticated apparatus, viability, easiness, and cheap are some advantages of this system (Burgess et al., 2013). For instance, Zhao and co-workers (2012) have established BSA-stabilized Au nanoclusters with intrinsic peroxidase-like activity for colorimetric detection of uric acid which displayed respectable outcomes with moderately great sensitivity. But, the interface of biothiols present in the biological samples with uric acid is the disadvantage of this procedure (Liu et al., 2011; Zhao et al., 2012; Wang et al., 2012).

To overcome these problems, researchers used the cascade approach of a combination of uricase and nanozyme for uric acid detection. For examples, Wu et al. (2015) established an operative sensing manner based on the distinctive optical properties of Ag nanoprisms. Hydrogen peroxide produced from uric acid oxidation by uricase, make about 120 nm blue shift in spectrum curve of surface plasmon resonance. Furthermore, Azmi et al. (2015) reported a sensing approach involving of uricase/HRP–CdS quantum dots (QDs) for the UA measurement in urine fluids. The QDs fluorescence was quenched by produced H_2O_2 which was related to the value of UA. To date, there are just a few reports about using metal organic framework (MOF) for uric acid sensing. Lu et al. (2015) used MIL-53(Fe) with peroxidase-like activity to develop an effective approach for colorimetric measurement of UA.

Metal organic frameworks are porous hybrid compounds which attract much attention due to their distinctive properties than other nanostructures, and have many applications in different fields such as industry, environment, and medicine. These compounds are biocompatible, biodegradable, as well as stable in different chemical environments which make these compounds to use for biological applications (Khan et al., 2015; Campbell et al., 2017; do Nascimento et al., 2017). So far, various metal-organic nanocompounds have been synthesized in different methods, among which ultrasonic method make the reaction occurs at ambient temperature, increases the yield of the product, and also promotes the synthesis speed of the materials. On the other hand, the reverse micelle method for synthesizing of these compounds, not only increase their stability but also synthesize a new product by controlling various properties (Esrafili et al., 2017; Sun et al., 2016). In general, if each of these methods is used separately, however, some of the properties of synthesized products such as surface area and thermal stability are highest than other methods, the characteristics of the obtained products are not very ideal to the purpose of industrial applications. For the first time in 2017, Sargazi and co-workers used ultrasonic method along with the reverse micelle method for synthesizing a new porous structure of Thorium and Tantalum nanomaterials that was the basis for extensive research, and finding a wide range of application of this compound (Sargazi et al., 2017, 2018). They used the 2^k factorial method for designing the experiments in which response surface methodology (RSM) predicted the possibility of formation of new samples with special properties.

In this study, according to the RSM predictions, Thorium compounds were synthesized by selecting the appropriate amounts of synthetic parameters with specific properties for use in biological fields. The obtained Th-MOF with extremely peroxidase-like activity used to oxidize the TMB substrate in the attendance of hydrogen peroxide, which presented an efficient and sensitive approach for uric acid detection. The Th-MOF morphology has been characterized. Peroxidase-like activity of Th-MOF has been described, and all parameters have been optimized in sensing of UA. Finally, the impact of this appreciated method for the UA measurement in human urine and serum fluids was successfully investigated. Consequently, our results indicated that this efficient, simple, precise, and sensitive UA sensor could be used in the clinical applications.

2. Materials and methods

2.1. Reagents and materials

Uricase from *Candida* sp. was obtained from Sigma-Aldrich and kept on at −20 °C refrigerator. 3,3′,5,5′- tetramethylbenzidine (TMB), and uric acid (UA) were acquired from Merck (USA). H_2O_2, sodium acetate, sodium dihydrogen phosphate, absolute ethanol, etc., were in analytical grade. Allopurinol (> 99%), and xanthine (> 99%), and Th $(NO_3)_4.5H_2O$ were also obtained from Sigma-Aldrich. Ultrapure water used for the making of solutions was manufactured by a Milli-Q water system (Millipore, Bedford, MA, USA). Human urine and serum fluids were gained from the Afzallipour Hospital, Kerman University of Medical Sciences (Kerman, Iran).

2.2. Synthesis of Th-MOF

The thorium-organic framework was prepared by ultrasound assisted reverse micelle (UARM) in which the reverse micelle system consisted of a surfactant and an organic solvent. Briefly, two solutions were separately prepared. Former, 0.0682 g of $Th(NO_3)_4.5H_2O$ salt (0.120 mmol) added in 20 mL of double-distilled water at the ambient temperature and later 0.0400 g of 2, 6- pyridine dicarboxylic acid (0.239 mmol) was dissolved in 5 mL of double-distilled water. Next, two above solutions combined. After that, the obtained solution was slowly added to a pyrex tube containing 6 mL of n-hexane and 0.02 g of sodium dodecyl sulfate (0.077 mmol) as the surfactant agent. This solution was stirred by a hot plate stirrer for 60 min at 80 °C. After 90 min, the process of reverse micelle system established well. Afterward, this solution was delivered into the ultrasound bath and the reaction was taken in special irradiation conditions (ultrasound duration = 21 min, temperature = 40 °C, and ultrasound power = 175 W). Afterward, the silvery product of Th-MOF was separated by the centrifugation and washed with DMF three times. The simple schematic of the construction of the porous Thorium-organic framework is presented in Scheme 1.

2.3. The catalytic activity of Th-MOF nanozyme

The peroxidase-like activity of Th-MOF nanozyme was investigated by catalytic oxidation of TMB in the presence of H_2O_2. Assay reaction consists of 470 μL of acetate buffer solution (100 mM, pH 5.5), 10 μL of TMB (10 mM, ethanol solution), 10 μL of hydrogen peroxide (0.1 mM) and 10 μL of Th-MOF dispersion (0.2 mg/mL) were added into 0.5 mL Eppendorf vial. The mixture was mixed, and incubated at 37 °C for 5 min and then the UV–vis spectra were observed using a UV–Vis spectrophotometer. The control sample containing all reagents expect Th-MOF. To find the optimal assay condition, the catalytic activity of Th-MOF nanozyme was considered at different condition. The assay was done at different concentrations of Th-MOF nanozyme from 0.005 to 0.8 mg/mL. Peroxidase-like activity of Th-MOF nanozyme was also considered at different pHs (2.5–8.5) and temperatures (20–80 °C) to obtain the best catalytic condition. To achieve the kinetic parameters of Th-MOF nanozyme, the catalytic activity was also considered at different concentrations of H_2O_2 (0.0–144 μM) and TMB (0.0–3000 μM).

2.4. Colorimetric detection of UA

UA was measured by catalytic activity of Uricase and Th-MOF nanozyme. Since the optimal activity of uricase was reported at pH 8.0, a stock solution of UA (1.5 mM) was equipped in 50 mM phosphate buffer solution (PBS, pH 8.0). Also, the optimal activity of Th-MOF was

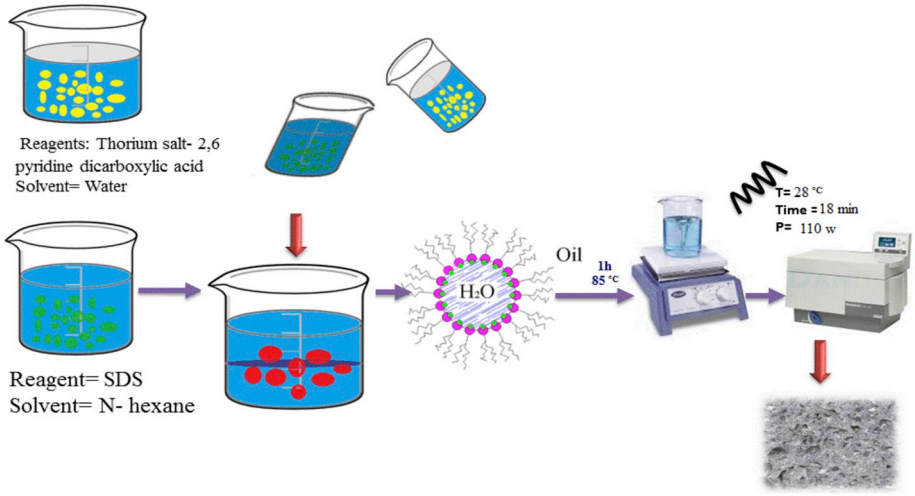

Scheme 1. Schematic representation of Th-MOF synthesized by ultrasound assisted reverse micelle method.

obtained in pH 5.5. So, a stock solution of Th-MOF (0.2 mg/mL) was prepared in acetate buffer (100 mM, pH 5.5). TMB (10 mM) was also prepared with absolute ethanol. The assay was done in two steps; at the first one, 100 µL of UA solution with different concentrations (or pre-treatment serum and urine samples) was mixed with 50 µL of 0.1 (mg/mL) Uricase and the mixture was incubated at 37 °C for 15 min. After that, in the second step, 470 µL of acetate buffer (100 mM, pH 5.5), 10 µL of TMB (10 mM), and 10 µL of Th-MOF dispersion (0.2 mg/mL) were added into the above reaction and incubated at 37 °C for 5 min. The color change from transparent to blue was observed at 652 nm by UV–vis spectroscopy. After confirming the function of this system, the effects of different concentrations of Uricase (0.00–0.033 mg/mL, final concentration) were also considered on UA sensing.

2.5. Determination of sensitivity and selectivity

To examine interference substrates present in normal human serum, some possible interfering materials (ascorbic acid, glucose, hypoxanthine, dopamine, xanthine, glutathione, histidine, proline, glycine, serine, valine, tryptophan, phenylalanine, and tyrosine) were selected

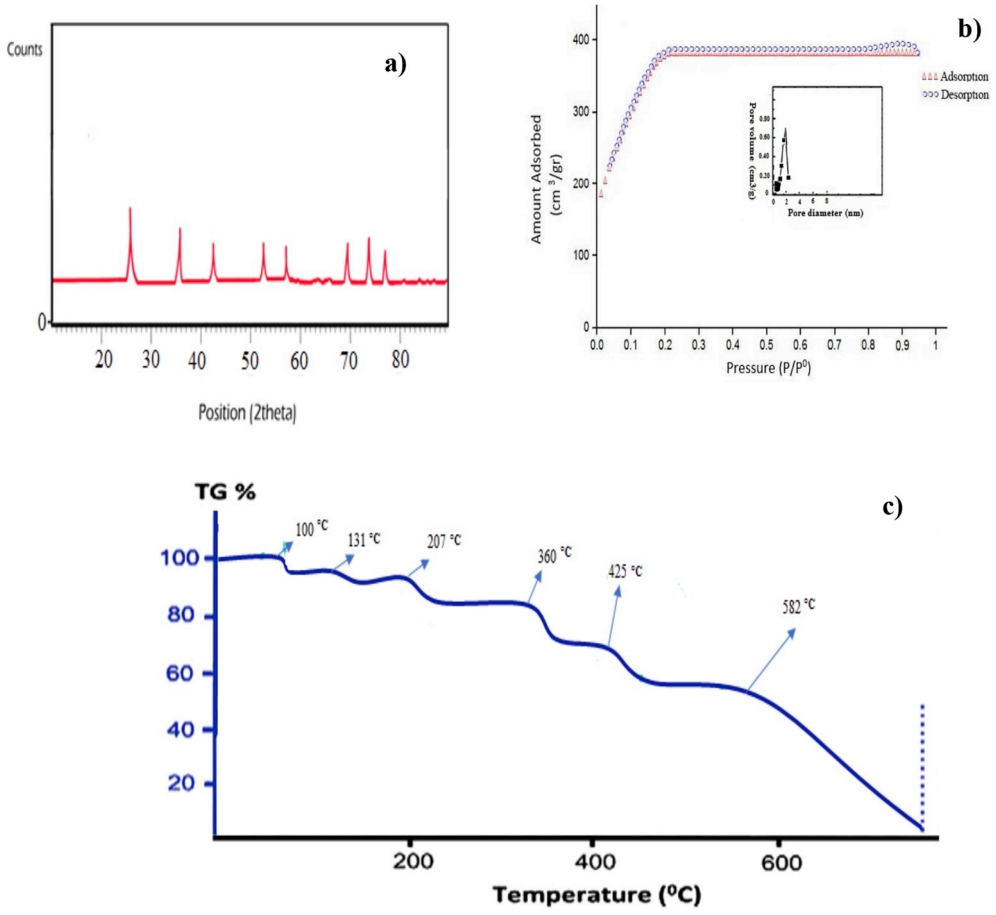

Fig. 1. XRD patterns (a), N2 adsorption/desorption (b) and TG analysis (c) of the Th-MOF.

and investigated in assay reaction. The volume and concentration of all reagents were the same as described in section 2.4., except instead of uric acid used 100 µl of the mentioned interfering materials (1.5 mM). Also, the selectivity of this sensing system was also investigated using two heterogeneous substrates allopurinol (> 99%) and xanthine (> 99%), which have chemical structures analogous to UA. The concentration and volume of these substrates analogous were the same as uric acid which described in section 2.4. For the selectivity examination, these two materials (allopurinol and xanthine) were also blended with UA (with the same concentration and volume as uric acid which described in section 2.4.), and the assay was done as described in section 2.4.

2.6. Biological samples collection and pretreatment

To investigate the bio-capacity of this system in real samples, we used this Uricase/Th-MOF catalyst system to quantity UA values in urine and serum trials. Human plasma and urine fluids were gathered from Afzalipour Hospital (Kerman, Iran). At first, plasma samples were centrifuged by 5000 rpm for 10 min to remove the large solid contents (proteins and red blood cells). The obtained supernatant was removed and transferred into standardized test tubes and further diluted with deionized water to eliminate the background color. The assay was done as described in section 2.4., except instead of uric acid used 100 µl of the diluted biological samples. The resulting UA values were multiplied in dilution factor (30 folds for serum samples and 25 folds for urine samples), and compared with those obtained from clinics. Furthermore UA values of the serum and urine trials were also measured using a standard curve. Different amounts of uric acid were blended to serum and urine samples, and finally, uric acid values in these samples were measured as described in section 2.4. The concentration of added uric acid was 10, 15 and 25 µM for serum samples and 8, 12 and 16 µM for urine samples, respectively. The recovery of the system was also measured as follow (Nikzad & karami, 2018):

Recovery (%): (increased UA concentration in the biological sample)/(added UA concentration) × 100

3. Results and discussion

3.1. MOF synthesis and characterization

Fig. 1a shows X-ray diffraction pattern of the metal-organic framework of Thorium synthesized by ultrasound assisted reverse micelle (UARM) which is in agreement with the diffraction patterns of the previous synthesized sample and confirms Th-MOF was well constructed (Sargazi et al., 2017). Also, according to the calculations obtained by Debye scherrer equation, the crystal size measured about 23 nm, which was nearly smaller than the sample synthesized in the previous work, and the percentage of crystallinity of the as-synthesized structure has also been improved (Sargazi et al., 2017). Also, the absorption and desorption behavior of the samples is shown in Fig. 1b. Based on the BET technique, the behavior of synthesized Th-MOF follows from the absorption type I absorption isotherm, Langmuir isotherm, which reveals that the structure has a microporous nature (Zou et al., 2017). Based on the calculations of this technique, the sample has a surface area of about 1350 m^2g^{-1}, which provides appropriate surface conditions for the use of this compound in the biological application.

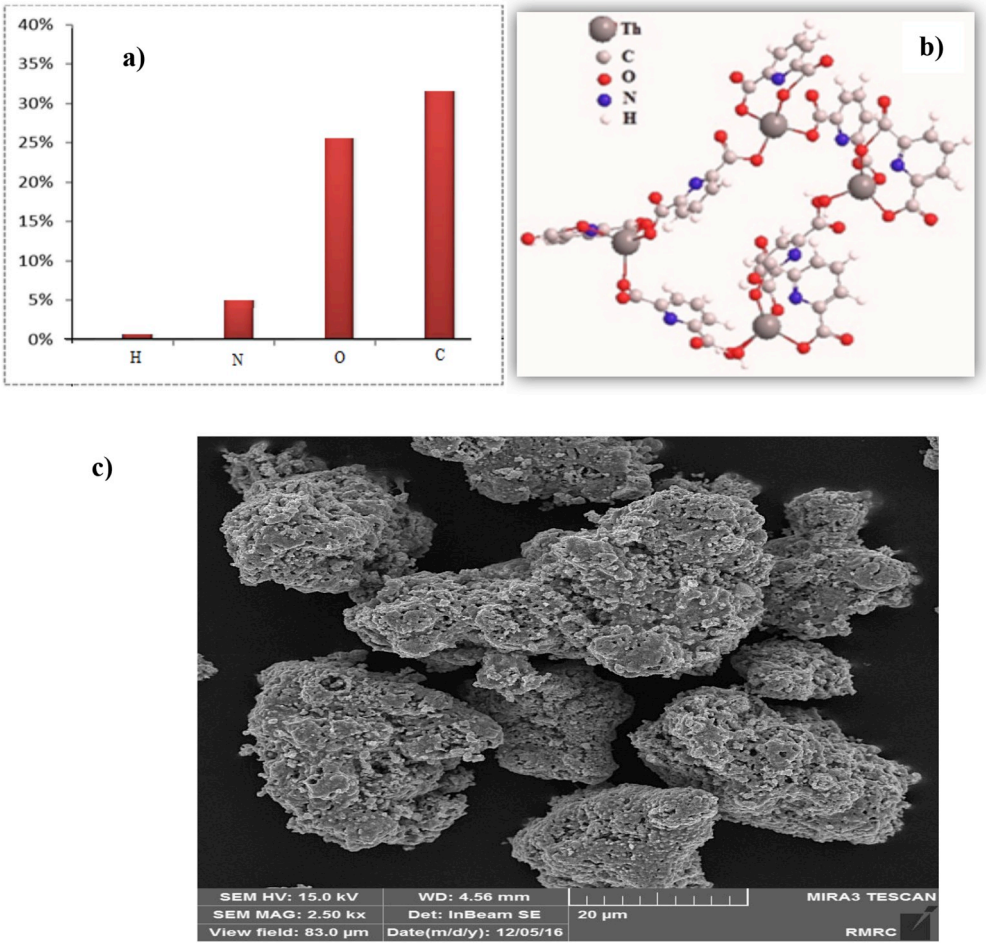

Fig. 2. CHNO analysis (a), suggested structure for Th-MOF (b), and SEM image of the Th-MOF synthesized by ultrasound assisted reverse micelle (c).

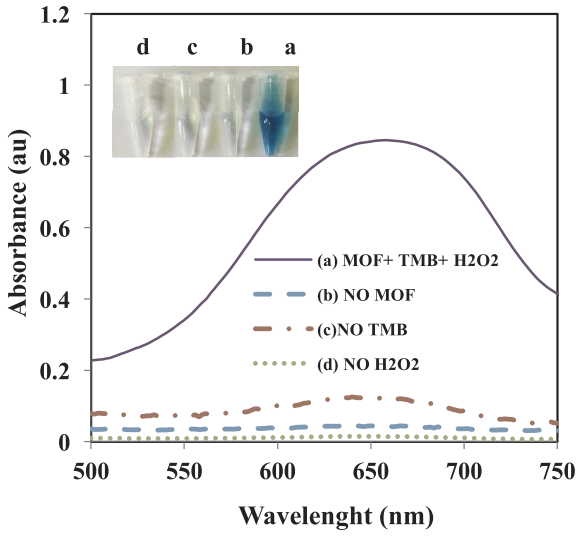

Fig. 3. (a) The UV/Visible absorption spectra of (a) catalytic reaction containing 470 µL of acetate buffer solution (100 mM, pH 5.5), 10 µL of TMB (10 mM, ethanol solution), 10 µL of hydrogen peroxide (0.1 mM) and 10 µL of Th-MOF dispersion (0.2 mg/mL) were added into 0.5 mL Eppendorf vial. The mixture was mixed, and incubated at 37 °C for 5 min. (b) containing all reagents except MOF, (c) containing all reagents except MOF and (d) containing all reagents except H_2O_2.

TGA and DTA analysis were used to determine the thermal stability of the synthesized sample. As shown in Fig. 1c, the sample has thermal stability up to 360 °C. To prepare the pure composition of the sample, the established micelle nonreactor should be destroyed, which occurs at a temperature of about 210 °C, according to the TGA analysis (Semino et al., 2017). Also, surface and trapped waters are removed at around 100 °C and 131 °C, respectively. To determine the elements in the final structure of the product, the elemental analysis of CHNO has been taken that values of each of these elements are shown in Fig. 2a, since the values are consistent with the values synthesized by sargazi et al. in the previous sample (Sargazi et al., 2017). Therefore, the final structure of porous nanomaterials is the same as the previous version as Fig. 2b. Morphology and size distribution of the final products is shown in Fig. 2c. According to this image, the sample has homogenous morphology without any agglomeration in the structure. Also, the average size distribution of the sample is 27 nm which confirms the nanostructure nature of the compound. The narrow size distribution of the product can be attributed to the effects of ultrasound assisted reverse micelle route (Sargazi et al., 2017).

3.2. Peroxidase-like activity of Th-MOF

To consider the peroxidase-like activity of the Th-MOF nanozyme, TMB oxidation was investigated in the attendance of H_2O_2. As shown in Fig. 3, the UV–vis spectra of the catalytic solution of TMB, Th-MOF, H_2O_2 in 100 mM acetate buffer (pH 5.5) was compared with control solutions. Also, the insertion is a picture of the four different reaction systems. These control solutions contain all reagents except Th-MOF, TMB, and H_2O_2 at different tests. A tense absorbance peak was established for TMB-H_2O_2 in the existence of Th-MOF with maximum absorbance at 652 nm (curve a). On the contrary, control solutions exhibited no absorbance at the same wavelength (curves b-d) which indicated that no oxidation reaction happened. These results reveal that Th-MOF displays excellent peroxidase-like activity, like generally used horseradish peroxidase (HRP). Free hydroxyl radicals (•OH) are significant intermediates in reactions including H_2O_2 (Dong et al., 2015a, b). Lu et al. (2015) indicated that the peroxidase-like activity of MIL-

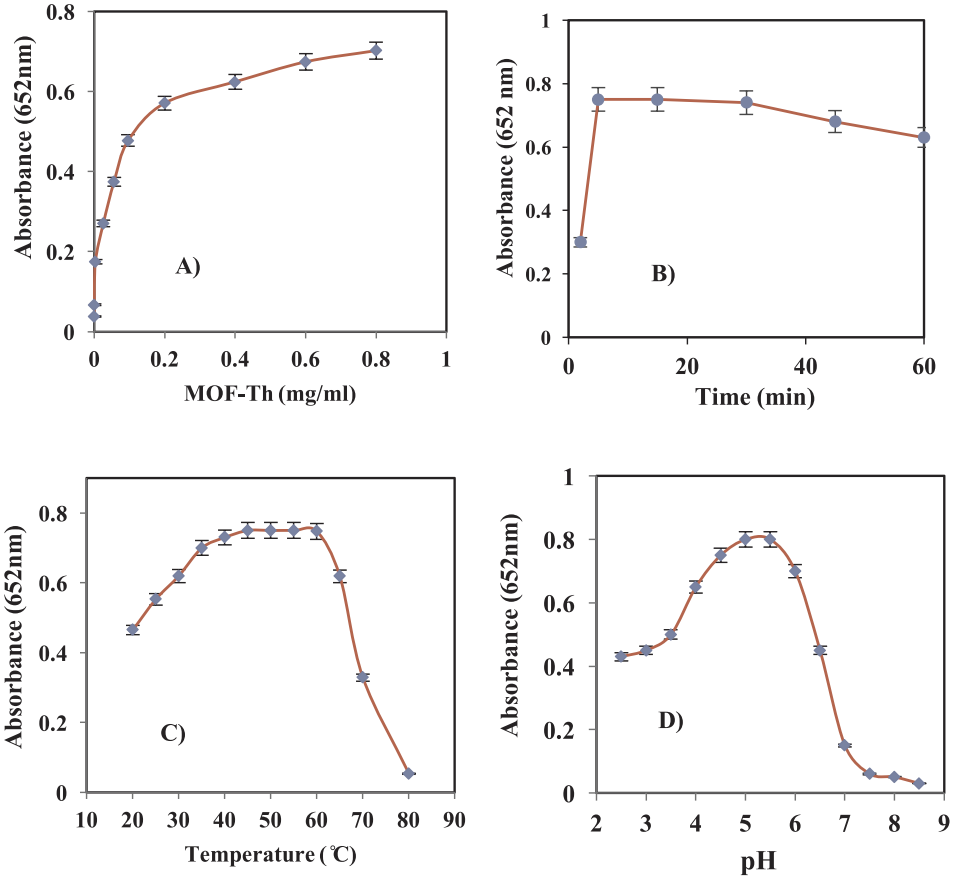

Fig. 4. Investigation of the different concentration of Th-MOF (0.005–0.8 mg/mL) on TMB oxidation (A). Investigation of the different time (2.0–60 min) on TMB oxidation (b), effect of the different temperatures (20–80 °C) (c) and pHs (2.5–8.5) (d) on the peroxidase-like activity of Th-MOF. Error bars show the standard deviation from three parallel measurements. The concentration and volume of the other reagents were the same as described in section 2.3.

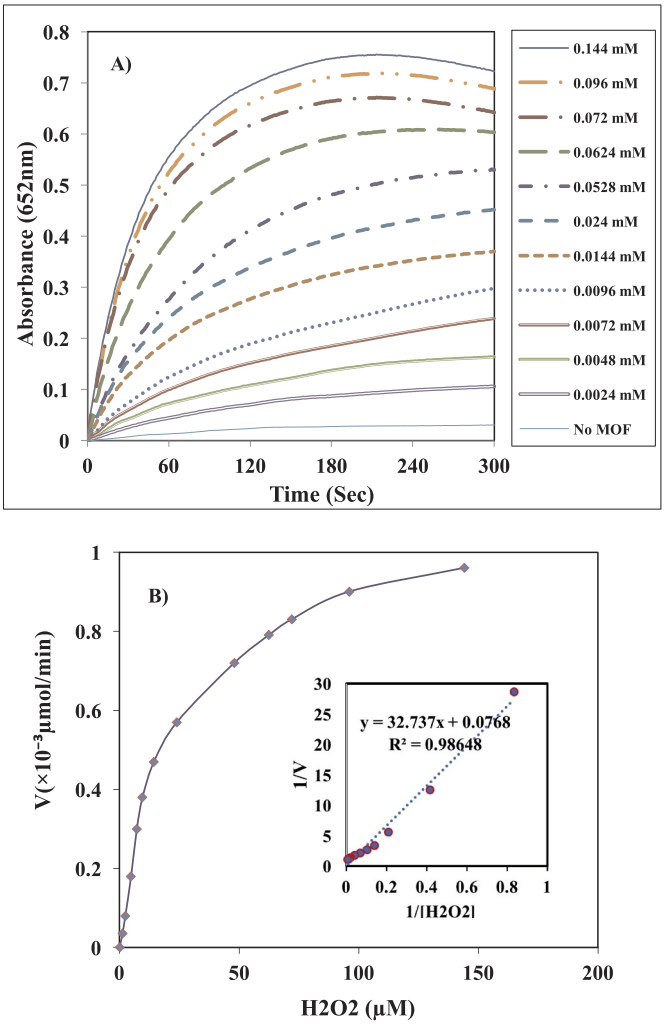

Fig. 5. A) Kinetic study of Th-MOF against different concentration of H_2O_2 (0.0–144 µM). B) Michaelis–Menten and Lineweaver–Burk curves of Th-MOF against the mentioned concentration of H_2O_2.

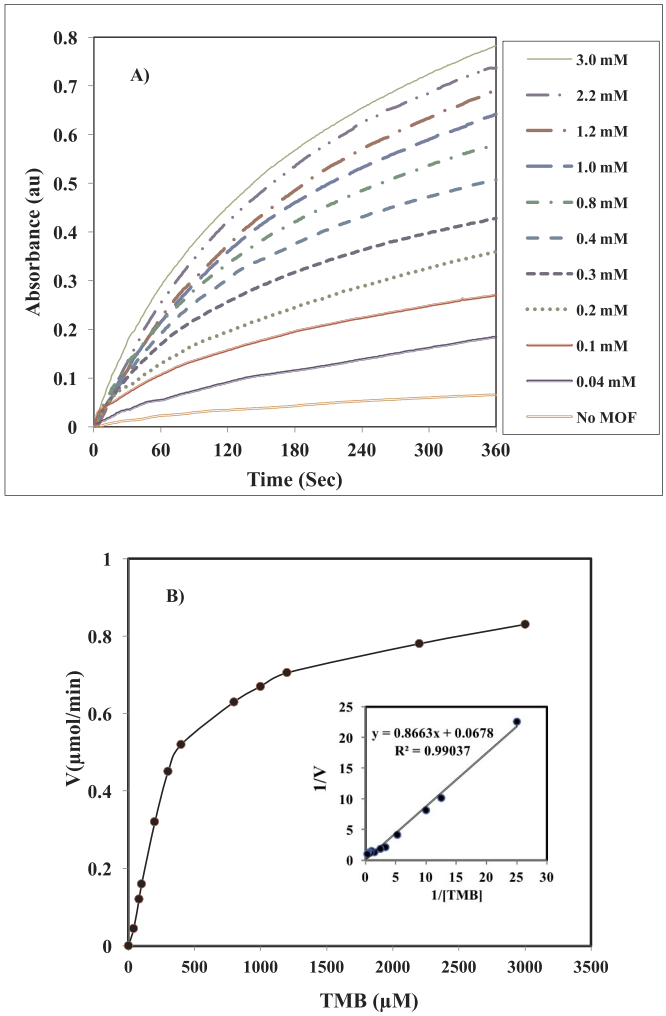

Fig. 6. A) Kinetic study of Th-MOF against the different concentration of TMB (0.0–3000 µM). B) Michaelis–Menten and Lineweaver–Burk curves of Th-MOF against the mentioned concentration of TMB. The concentration and volume of the other reagents were the same as described in section 2.3.

53(Fe) could be ascribed to their metal (Fe) centers. Furthermore, the TMB substrate can probably adsorb on the superficial of MIL-53(Fe) through the hydrogen bonding and π-π interactions (Lu et al., 2015). Finally, the newly designed Th-MOF has excellent peroxidase-like activity because of its significant catalytic efficiency to decompose hydrogen peroxide into hydroxyl radicals (Wu et al., 2017).

3.3. Optimization of colorimetric analysis conditions

The catalytic activity of Th-MOF was considered under diverse pH, time, Th-MOF concentrations, and temperatures. The value of Th-MOF was also investigated from 0.005 to 0.8 mg/mL in assay condition. Results showed that the activity was improved sharply up to 0.2 mg/mL, after that the activity was increased slowly. For the following studies, the amount of Th-MOF was 0.2 mg/mL (Fig. 4A). Results of time investigation of Th-MOF activity in Fig. 4B shown that oxidation reaction was finished after 5 min of incubation, represent that TMB oxidation by Th-MOF in the existence of hydrogen peroxide molecules showing a fast rate. In comparison, Fe_3O_4@MIL-100(Fe) showed maximum peroxide mimicking activity after 15 min of incubation (Wu et al., 2017).

As shown in Fig. 4C, the peroxidase-like activity of Th-MOF was increased with the rise of temperature and maximum activity was obtained from 40 to 60 °C. Also, the activity was sharply decreased at higher temperatures. Therefore, in the following studies, the catalytic assay was done at 40 °C. In the previous reports suggested that in the higher temperatures the diffusion, kinetic energy of hydrogen peroxide, and also the collisions increased between hydrogen peroxide and the catalytic sites of Th-MOF. But, in the temperatures above 55 °C, hydrogen peroxide molecules decompose to other products such as hydroxyl radicals before it reacts to the catalytic sites of Th-MOF (Wu et al., 2017; Lu et al., 2015). The effects of pH amounts are revealed in

Table 1
Maximum reaction rate (Vm) and Michaelis–Menten constant (*K*m) for applied peroxidase-like nanomaterials compared with HRP.

Catalyst	*K*m [mM]		Vm [10^{-8} M s^{-1}]		References
	TMB	H_2O_2	TMB	H_2O_2	
Th-MOF	0.012	0.426	24.56	21.70	Present study
Fe3O4@MIL-100(Fe)	0.112	0.077	11.42	17.95	Wu et al. (2017)
MIL-53(Fe)	1.080	0.040	8.780	1.860	Qin et al. (2013)
Memin@MIL-101(Al)–NH2	0.068	10.90	6.070	8.980	Ai et al. (2013)
Fe_3O_4	0.098	154.0	3.440	9.780	Dong et al., 2015a, b
HRP	0.434	3.700	10.00	8.710	Dong et al., 2015a, b

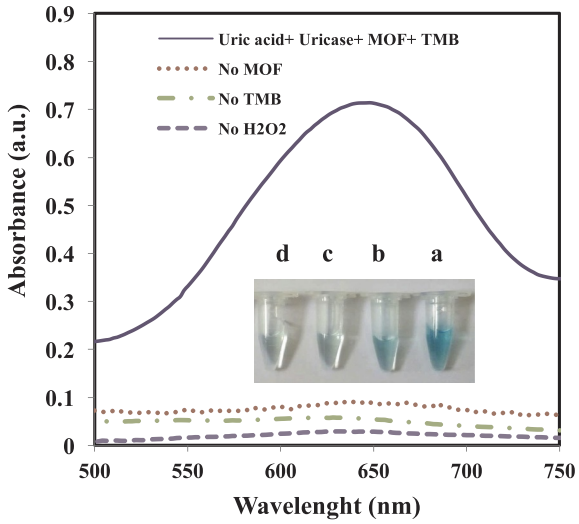

Fig. 7. To confirm the application of uricase/Th-MOF system for uric acid sensing, the assay was done in two steps; at the first one, 100 μL of UA solution was mixed with 50 μL of 0.1 (mg/mL) Uricase and the mixture was incubated at 37 °C for 15 min. After that, in the second step, 470 μL of acetate buffer (100 mM, pH 5.5), 10 μL of TMB (10 mM) and 10 μL of Th-MOF dispersion (0.2 mg/mL) were added into the above reaction and incubated at 37 °C for 5 min. (a) containing all reagents, (b) containing all reagents except MOF, (c) containing all reagents except TMB, (d) containing all reagents except MOF H_2O_2.

Fig. 4D. The peroxidase-like activity of Th-MOF was highest at pH 5.0–5.5. However, the activity of Th-MOF was decreased when pH raises to acidic and alkaline values. Consequently, for the following studies pH 5.5 was chosen for consideration of MOF activity. These results are similar to the activity of MIL-53(Fe) which displays higher operative catalytic sites at acidic pH (Lu et al., 2015; Su et al., 2012; Chen et al., 2013; Wu et al., 2017). Taken to gather, these results indicating that Th-MOF has excellent peroxidase mimetics.

3.4. Steady-state kinetic assay of Th-MOF

Kinetic parameters of peroxidase-like activity of Th-MOF were considered using steady-state kinetics. As shown in Figs. 5 and 6, the plots of initial velocity against different concentrations of hydrogen peroxide and TMB monitored classic Michaelis–Menten manners. Lineweaver–Burk plots were also used to acquire the Michaelis–Menten constant:

$$\frac{1}{v} = \frac{K_m}{V_m}\left(\frac{1}{[S]} + \frac{1}{K_m}\right)$$

Where [S] resembles the substrate concentration, *K*m is the Michaelis–Menten constant, V_0 is the initial velocity of reaction, and Vm signifies the maximal velocity of TMB oxidation. Table 1 shows the amount of *K*m and Vm for TMB and hydrogen peroxide. It is mentioned that *K*m is a sign of enzyme affinity to substrates (TMB/H_2O_2). A high value of *K*m signifies a weak affinity and vice versa (Liu et al., 2011). Comparison in Table 1 showed that *K*m value of Th-MOF with TMB as substrate is much lower than that of the other mentioned catalysts. For instance, *K*m values of Th-MOF with TMB is lower than 9.3 folds in comparison with *K*m values of Fe3O4@MIL-100(Fe) (Wu et al., 2017). Furthermore Th-MOF was also showed higher Vmax values in comparison with the other catalysts. For example, Vmax value of Th-MOF was obtained about 2.15 folds more than Vmax values of Fe3O4@MIL-100(Fe) (Table 1). These results indicated the high impact of this Th-MOF nanozyme catalyst in peroxidase mimicking

3.5. Quantitative determination of UA

As we previously mentioned, hydrogen peroxide produced from UA oxidation as a result of uricase activity. Also, the absorbance of oxidized TMB solution in assay reaction is linearly related to hydrogen peroxide concentration. Consequently, the suggested colorimetric manner (Th-MOF/uricase) could be used to quantitatively measurement of UA values. Fig. 7 shows the excellence UV–visible curve of uric acid sensing system (containing uric acid, uricase, Th-MOF, and TMB). No obvious peak is seen in three control samples which indicated the specificity of this sensing system. In this system, H_2O_2 which produced from uricase action on uric acid was used as a substrate of Th-MOF to produced OH radical. Finally, the produced radical oxidized TMB with blue color.

Fig. 8A shown the absorbance values of the oxidized TMB at different UA concentrations. Results showed that the absorbance value amplified progressively with increasing the UA concentration from 0 to 1000 μM (Fig. 8B). As shown in Fig. 8C, with increasing in uric acid concentration blue color of sensing system regularly developed and can be detected by the naked eye. The linear regression equation for uric acid substrate was stated as A = 0.0039C + 0.0519 with a correlation coefficient of 0.9955 (Fig. 8b inset), where C is the uric acid concentration, A express the absorbance value. The linear range for uric acid was from 4.0 to 70 μM, and the LOD was measured as 1.15 μM. Furthermore the LOD and linear range of UA detection have been compared with the previous reports. As we can be seen in Table 2, the suggested manner shows some advantages compared to the other reports, except Uricase/BSA-stabilized Au nanoclusters. In spite of that, in the mentioned method, biothiols present in serum showed intense interactions with Au nanoclusters via Au–S bonds, affecting the reducing of catalytic activity. In summary, this colorimetric system (Th-MOF/Uricase) presented a moderately low LOD and good linear range which was proper for clinical applications.

3.6. Investigation of uricase concentrations on the catalytic system

The value of the final concentration of uricase in assay solution was also considered from 0.002 to 0.033 (mg/ml). Results in Fig. 9A showed that the activity was linearly increase up to 0.033 (mg/ml), and after that it was constant. For the following studies, the amount of uricase was 0.033 (mg/ml).

3.7. Investigation of Th-MOF reusability

The reusability of Th-MOF catalytic system was also investigated using the same amount of UA in the similar sets of the assay for seven cycles (Fig. 9B). At the end of each assay, the Th-MOF catalyst was separated by centrifugation from the assay solution and washed with distilled water. After that, the MOF catalyst was dried at 37 °C beforehand subsequent cycle. Results in Fig. 9B shown, the absorbance of assay reaction was approximately constant in the following four cycles, demonstrating that Th-MOF catalyst has outstanding stability. It is mentioned that the activity was about 85% after seven cycle reuse.

3.8. Interference experiments

Selectivity is a chief issue for gaging the biosensor action. To consider the selectivity of UA revealing by using Th-MOF as peroxidase mimic, the absorbance values of this bio-sensing system were determined for other interface substances which might be present in serum samples. Results in Fig. 10A, shown that the public interfering substances had no obvious absorbance values and it was less than 0.1. The absorbance of blue color oxTMB diminished in the attendance of ascorbic acid, citric acid, cysteine, albumin, glycine and their mixture (without UA) which it is similar to previous reports (Lu et al., 2015). Conversely, when the UA added to the mixture of all interfering substances a strong absorbance value was observed. Consequently, the

suggested system based on Th-MOF catalytic displayed high selectivity for UA measurement in urine and serum samples.

Also, the Uricase–MOF catalyst system presented significantly high selectivity concerning UA in contrast to other related complexes.

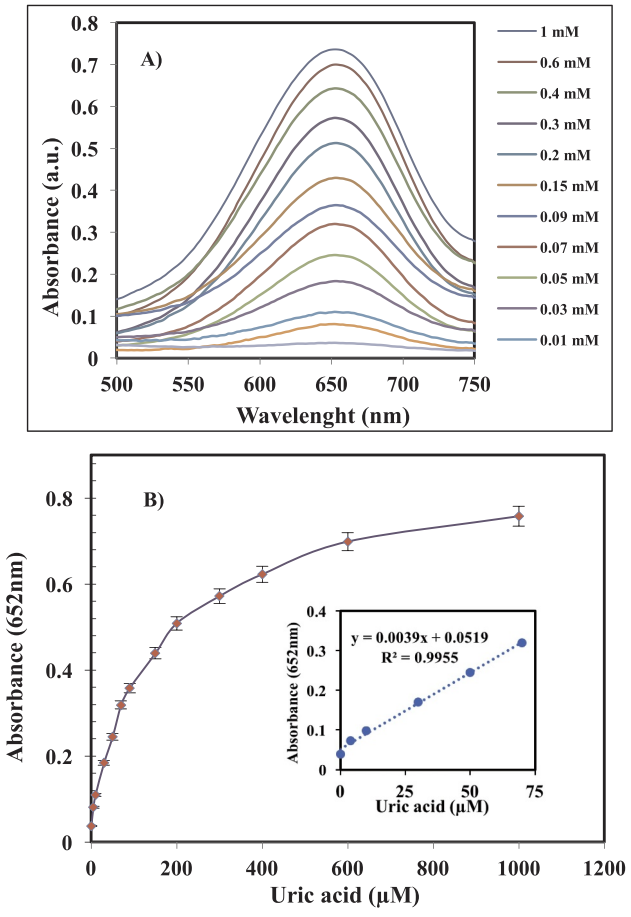

Fig. 8. (a) The UV/Visible absorption curves of the colorimetric sensing of different concentrations of UA (0.0–1000 µM). (b) A dose-response curves for UA measurement in the range of 0–1000 µM using Th-MOF as a peroxidase mimic. Inset: The linear tuning plot for UA substrate. Error bars expression the standard deviation from three equivalent tests. (c) Image of colored products with increasing the UA concentrations (From left to right). The concentration and volume of all reagents were the same as described in section 2.4.

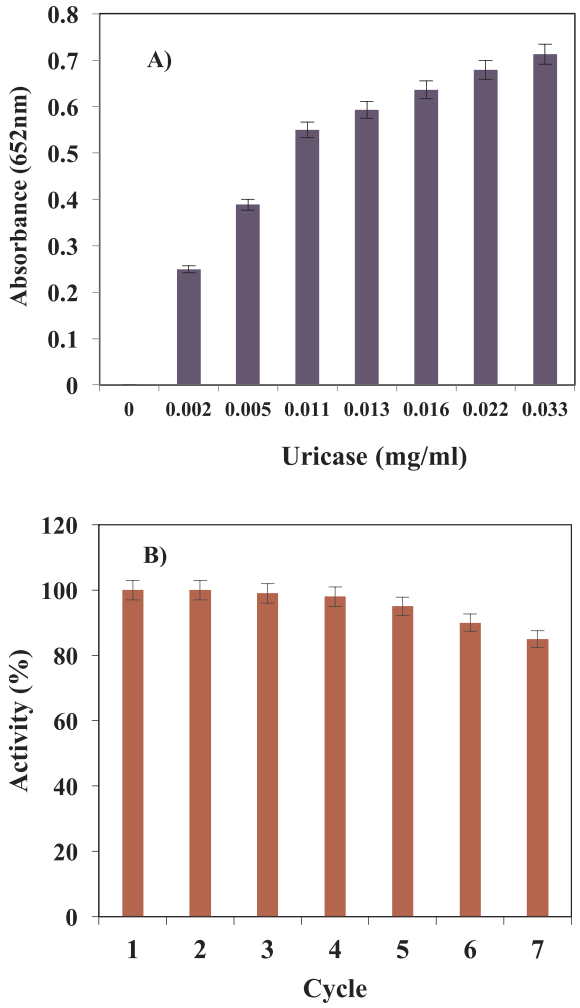

Fig. 9. (a) Investigation of UA sensing system in the presence of different concentration of uricase from 00.2 to 0.033 (mg/ml). (b) Recyclability experiments of Th-MOF catalyst in the Uricase/Th-MOF system were also evaluated. After each cycle the reaction was centrifuged, the pellet (Th-MOF) was washed with distilled water and assayed in the next cycle. The concentration and volume of all reagents (except Th-MOF) were the same as described in section 2.4.

Allopurinol and xanthine which have purine base structures analogous to UA were selected to examine alone and in blend with UA to consider the selectivity of the Uricase–MOF sensing system (Fig. 10B). Results in Fig. 10C shown that the reaction proceeded just in the present of UA and there is not any obvious color in the absent of UA. Kim and co-workers (2016) also reported that, the same results for the cascade determination of uric acid by biomimetic peroxidase-like catalyst (PMOx) and Uricase (Kim et al., 2016). Consequently, these results indicated that the high selectivity of Uricase–MOF sensing system concerning UA over other related complexes.

Table 2
Comparison of detection limits (LOD) and linear range for Uricase/MOF-Th system with other analytical methods.

Analytical method	Linear range (µM)	Detection limit (µM)	References
Luminol-K_3 [Fe (CN)6]	4.8–179	3.0	He et al. (2005)
Uricase/AuNP/MWCNT Au electrode	10–800	10.0	Chauhan and Pundir (2011)
Uricase/BSA-stabilized Au nanoclusters	2.0–200	0.36	Zhao et al. (2012)
Uricase/HRP-Cds quantum dots	125–1000	125	Azmi et al. (2015)
Uricase/MIL-53(Fe)	4.5–60	1.3	Lu et al. (2015)
Uricase/MOF-Th	4.0–70	1.15	Present study

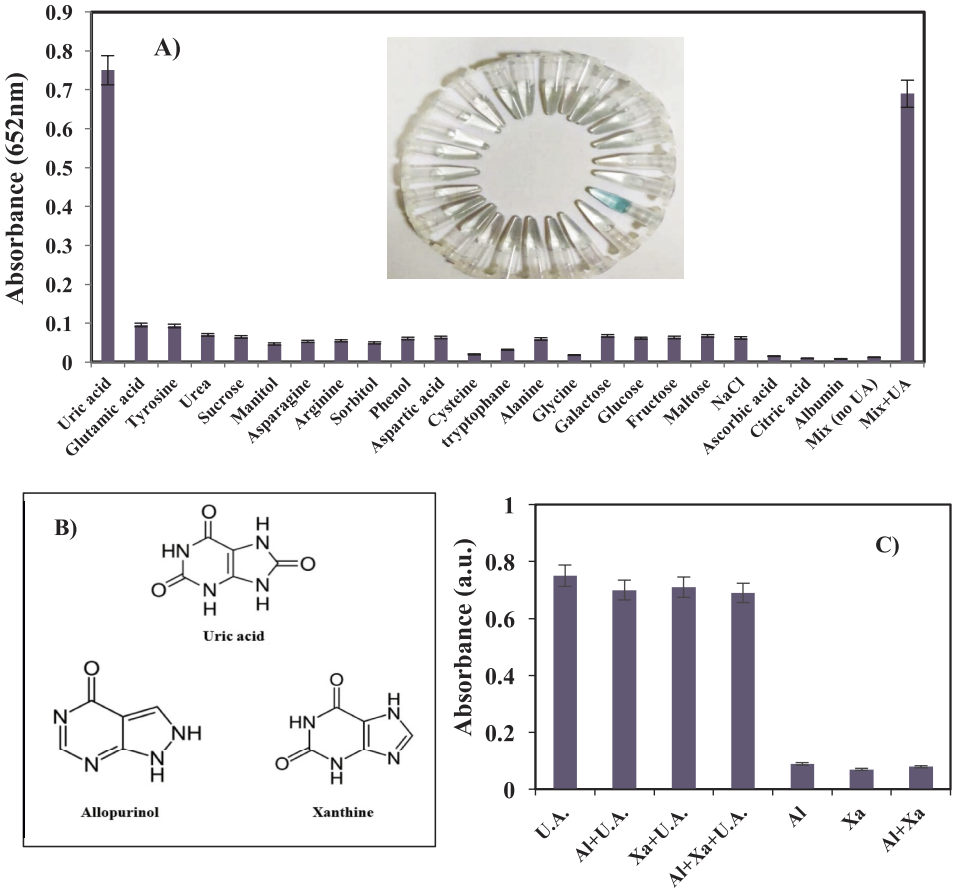

Fig. 10. (a) Absorbance response of the colorimetric sensing system in the presence of some interfacing substrates. The concentration and volume of all reagents were the same as described in section 2.5, except, 100 μL of interfacing substrates (1.5 mM) used instead of UA. Error bars indication the standard deviation from three equivalent tests. (b) Structures of uric acid analogues. (c) The selectivity test was also investigated in the presence of some uric acid analogues (Xanthine (Xa) and Allopurinol (Al)) alone and the combination with UA, with the same concertation as UA. The concentration and volume of all reagents were the same as described in section 2.4.

Table 3
Determination of UA in human serum and urine samples.

Samples	Founded (μM)	Value of this method	Value of clinical method	Added (μM)	Detected (μM)	Recovery (%)	RSD (n = 3, %)
Serum 1	19.65	585.5	578.1	10.0	28.96	93.10	2.6
				15.0	34.16	96.73	1.3
				25.0	43.71	96.24	2.1
Serum 2	20.18	602.3	597.2	10.0	30.11	99.30	3.8
				15.0	34.98	98.66	2.1
				25.0	44.94	99.04	1.8
Serum 3	22.03	652.1	650.2	10.0	31.67	96.40	4.3
				15.0	35.86	92.20	2.7
				25.0	46.74	98.84	3.2
Urine 1	24.34	603.5	–	8.0	32.13	97.37	1.1
				12.0	35.80	95.50	1.9
				16.0	40.60	101.62	2.6
Urine 2	20.61	512.25	–	8.0	28.60	99.87	4.1
				12.0	31.80	93.25	3.6
				16.0	36.12	96.93	3.1
Urine 3	22.26	551.5	–	8.0	30.20	99.25	1.2
				12.0	34.14	99.00	2.3
				16.0	37.70	96.50	2.4

3.9. Detection of UA in serum and urine samples

The offered sensing method was used to the UA measurement in serum and urine samples under the optimum experimental environments. Three serum and urine samples were acquired from a clinic. The UA values of samples measured by the MOF-uricase sensing system are listed in Table 3. For the measurement of UA in these real samples, a standard addition technique was also used, and the evaluated samples were jagged by three diverse values of standard UA solution. Results in Table 3 show the recoveries for UA in serum fluids were between 93.10% and 99.04%. The relative standard deviation (RSD, n = 3) at each concentration value was less than 4.3%. Furthermore results also show, the recoveries for UA in urine samples were between 93.25% and 101.62%. The relative standard deviation (RSD, n = 3) at each concentration value was less than 4.1%. All these results directed that Th-MOF was a talented nano-material as artificial peroxidase in UA measurement. Lu and co-workers (2015) reported that recoveries of UA measurement by uricase/MIL-53(Fe) in human urine samples were from 89.50 to 99.38%, whereas the recoveries for serum trials were gained from 93.70 to 101.44%. The RSD parameter was also obtained less than 4.8% (Lu et al., 2015).

To check additional the precision of the MOF-Uricase sensing

system and the constancy of the reaction assay system, UA determination in serum fluids has been confirmed through comparison between the recommended technique and tedious clinical approaches. The obtained results in Table 3 show that the UA concentrations in serum 1, 2 and 3 were 585.5, 597.2 and 650.2 μM, respectively, which show reliability with the values calculated by the clinical approaches in the clinical laboratory (serums 1, 2 and 3 were 578.1, 597.2 and 650.2 μM, respectively). Good recovery and accuracy of UA measurement indicated that this established colorimetric sensing system is appropriate for UA revealing in actual experimental samples.

4. Concluding remarks

In this study, a novel MOF composed of Thorium has been synthesized and characterized. Our results indicated that Th-MOF showed the appreciated the peroxidase-like activity and its catalytic activity was reliant on the reaction pH and temperature similar to natural HRP. As a mimic peroxidase, the Th-MOF displayed numerous advantages, such as stability, high catalytic efficiency, easy preparation and inexpensive. An efficient and facile colorimetric sensing method for UA determination in human serum and urine fluids was investigated by coupling of uricase and Th-MOF. Results indicated that this peroxidase mimicking MOFs nanozyme is a talented candidate for bio-sensing of UA in real samples especially in point of care diagnostic.

CRediT authorship contribution statement

Arastoo Badoei-dalfard: Conceptualization, Methodology, Validation, Supervision, Writing - review & editing. **Nasrin Sohrabi:** Data curation, Methodology, Validation. **Zahra Karami:** Supervision, Methodology, Validation, Writing - review & editing. **Ghasem Sargazi:** Data curation, Methodology, Writing - original draft.

Acknowledgment

The authors express their gratitude to the Research Council of the Shahid Bahonar University of Kerman, Kerman (Iran) for financial support during this project.

References

Ai, L., Li, L., Zhang, C., Fu, J., Jiang, 2013. J. Chem. 5 Eur. J. 19, 15105–15108.
Azmi, N.E., Ramli, N.I., Abdullah, J., Hamid, M.A.A., Sidek, H., Rahman, S.A., Ariffin, N., Yusof, N.A., 2015. Biosens. Bioelectron. 67, 129–133.
Bainbridge, S.A., Roberts, J.M., 2008. Placenta 29 (Suppl. ment), 67–72.
Boughton, J.L., Robinson, B.W., Strein, T.G., 2002. Electrophoresis 23, 3705–3710.
Burgess, I.B., Lončar, M., Aizenberg, J., 2013. J. Mater. Chem. C 1, 6075–6086.
Campbell, J., Tokay, B., 2017. Microporous Mesoporous Mater. 251, 190–199.
Cannon, P.J., Stason, W.B., Demartini, F.E., Sommers, S.C., Laragh, J.H., 1966. Engl. N., J. Med. 275, 457–464.
Chaudhari, R.D., Joshi, A.B., Srivastava, R., 2012. Sens. Actuators, B 173, 882–889.
Chauhan, N., Pundir, C.S., 2011. Anal. Biochem. 413, 97–103.
Chen, Y., Cao, H., Shi, W., Liu, H., Huang, Y., 2013. Chem. Commun. 49, 5013–5015.
Dawson, J., Walters, M., 2006. Br. *J. Clin. Pharmacol.* 62, 633–644.
do Nascimento, J.F.S., Barros, B.S., Kulesza, J., de Oliveira, J.B.L., Leite, A.K.P., de Oliveira, R.S., 2017. Mater. Chem. Phys. 190, 166–174.
Dong, W., Liu, X.D., Shi, W., Huang, Y., 2015a. RSC Adv. 5, 17451–17457.
Dong, Y.M., Zhang, J.J., Jiang, P.P., Wang, G.L., Wu, X.M., Zhao, H., Zhang, C., 2015b. New J. Chem. 39, 4141–4146.
Esrafili, L., Tehrani, A.A., Morsali, A., 2017. Ultrason. Sonochem. 39, 307–312.
Falasca, G.F., 2006. Clin. Dermatol. 24, 498–508.
Fang, J., Alderman, M.H., 2000. J. Am. Med. Assoc. 283, 2404–2410.
Gagliardi, A.C.M., Miname, M.H., Santos, R.D., 2009. Atherosclerosis 202, 11–17.
Grabowska, I., Chudy, M., Dybko, A., Brzozka, Z., 2008. Sens. Actuators, B 130, 508–513.
He, D., Zhang, Z., Huang, Y., Hu, Y., Zhou, H., Chen, D., 2005. Luminescence 20, 271–275.
Jen, J., Hsiao, S., Liu, K., 2002. Talanta 58, 711–717.
Johnson, R.J., Kang, D.-H., Feig, D., Kivlighn, S., Kanellis, J., Watanabe, S., Tuttle, K.R., Rodriguez-Iturbe, B., Herrera-Acosta, J., Mazzali, M., 2003. Hypertension 41, 1183–1190.
Jossa, F., Farinaro, E., Panico, S., Krogh, V., Celentano, E., Galasso, R., Mancini, M., Trevisan, M., 1994. J. Hum. Hypertens. 8, 677–681.
Kand'a´ r, R., ˇZa´kova´, P., Muz´a´kova´, V., 2006. Clin. Chim. Acta 365, 249–256.
Khan, N.A., Jhung, S.H., 2015. Coord. Chem. Rev. 285, 11–23.
Kim, M.C., Kwak, J., Lee, S.Y., 2016. Sens. Actuators, B 232, 744–749.
Kumar, A.S., Shanmugam, R., 2011. Anal. Methods 3, 2088–2094.
Liao, L., Liao, C., Liu, C., Yang, T., Wang, G., 2014. Clin. Chim. Acta 436, 72–77.
Lippi, G., Montagnana, M., Franchini, M., Favaloro, E.J., Targher, G., 2008. Clin. Chim. Acta 392, 1–7.
Liu, D., Wang, Z., Jiang, X., 2011. Nanoscale 3, 1421–1433.
Lohsoonthorn, V., Dhanamun, B., Williams, M.A., 2006. Arch. Med. Res. 37, 883–889.
Lu, J., Xiong, Y., Liao, C., Ye, F., 2015. Anal. Methods 7, 9894–9899.
Matějčková, J., Tůma, P., Samcová, E., Zemanová, Z., 2007. J. Sep. Sci. 30, 1947–1952.
Merriman, T.R., Dalbeth, N., 2011. Jt. Bone Spine 78, 35–40.
Moccia, M., Lanzillo, R., Palladino, R., Russo, C., Carotenuto, A., Massarelli, M., Vacca, G., Vacchiano, V., Nardone, A., Triassi, M., Morra, V.B., 2015. Clin. Chem. Lab. Med. 53, 753–759.
Nakagawa, T., Kang, D.-H., Feig, D., Sanchez-Lozada, L.G., Srinivas, T.R., Sautin, Y., Ejaz, A.A., Segal, M., Johnson, R.J., 2006. Kidney Int. 69, 1722–1725.
Nikzad, N., Karami, Z., 2018. Int. J. Biol. Macromol. 115, 1241–1248.
Nyhan, W.L., 1997. J. Inherit. Metab. Dis. 20, 171–178.
Perelló, J., Sanchis, P., Grases, F., 2005. J. Chromatogr. B 824, 175–180.
Qin, F., Jia, S., Wang, F., Wu, S., Song, J., Liu, Y., 2013. Catal. Sci. Technol. 3, 2761–2768.
Rocha, D.L., Rocha, F.R.P., 2010. Microchem. J. 94, 53–59.
Sargazi, G., Afzali, D., Mostafavi, A., 2017. Ultrason. Sonochem. 41, 234–251.
Sargazi, G., Afzali, D., Khajeh-Ebrahimi, Badoei-dalfard, A., Malekabadi, S., Karami, Z., 2018. Mater. Sci. Eng. C 93, 768–775.
Semino, R., Ramsahye, N.A., Ghoufi, A., Maurin, G., 2017. Microporous Mesoporous Mater. 254, 184–191.
Shen, L., Ji, H.F., 2013. BMJ Open 3, e003620.
Su, L., Feng, J., Zhou, X., Ren, C., Li, H., Chen, X., 2012. Anal. Chem. 84, 5753–5758.
Sun, W., Zhai, X., Zhao, L., 2016. Chem. Eng. J. 289, 59–64.
Wang, S., Chen, W., Liu, A., Hong, L., Deng, H.H., Lin, X., 2012. ChemPhysChem 13, 1199–1204.
Wang, J., Chang, Y., Wu, W.B., Zhang, P., Lie, S.Q., Huang, C.Z., 2016. Talanta 152, 314–320.
Wu, D., Lu, H.F., Xie, H., Wu, J., Wang, C.M., Zhang, Q.L., 2015. Sens. Actuators, B 221, 1433–1440.
Wu, Y., Ma, Y., Xu, G., Wei, F., Ma, Y., Song, Q., Wang, X., Tang, T., Song, Y., Shi, M., Xu, X., Hu, Q., 2017. Sens. Actuators, B 249, 195–202.
Zhang, J., Zhang, H., Du, Z., Wang, X., Yu, S., Jiang, H., 2014. Chem. Commun. 50, 1092–1094.
Zhao, J., 2013. Anal. Methods 5, 6781–6787.
Zhao, H., Wang, Z., Jiao, X., Zhang, L., Lv, Y., 2012. Spectrosc. Lett. 45, 511–519.
Zhou, S., Zuo, R., Zhu, Z., Wu, D., Vasa, K., Deng, Y., Zuo, Y., 2013. Anal. Methods 5, 1307–1311.
Zinellu, A., Carru, C., Sotgia, S., Deiana, L., 2004. Anal. Biochem. 330, 298–305.
Zou, Z., Li, S., He, D., He, X., Wang, K., Li, L., Yang, X., Li, H., 2017. J. Mater. Chem. B. 5, 2126–2132.